Int. J. Heat Mass Transfer. Vol. 19, pp. 277–283. Pergamon Press 1976. Printed in Great Britain

COMBINED FREE AND FORCED LAMINAR CONVECTION IN INCLINED RECTANGULAR CHANNELS

JENN-WUU OU, K. C. CHENG and RAN-CHAU LIN
Department of Mechanical Engineering, University of Alberta, Edmonton, Alberta, Canada

(*Received* 16 *July* 1974 *and in revised form* 20 *May* 1975)

Abstract—Fully developed combined free and forced laminar convection with upward flow in inclined rectangular channels under the thermal boundary condition of axially uniform wall heat flux or constant wall temperature gradient is studied by a numerical method using an improved formulation where three independent physical parameters Pr, Re_0^*, Ra^* appear instead of four in the previous investigations dealing with the inclined circular tubes. Numerical results for friction factor and Nusselt number are presented for $Pr = 5$ and aspect ratios $\gamma = 0{\cdot}5$, 1, 2. The new parameters are also used in correlating the previous flow and heat-transfer results for inclined tubes. The inclination angle effect is found to be most significant near the horizontal orientation and decreases as vertical direction is approached. At higher Ra^*, for example $Ra^* = 10^4$ for $\gamma = 1$, $Pr = 5$, the flow and heat-transfer results become independent of Re_0^* and the asymptotic behavior appears.

NOMENCLATURE

A, axial pressure gradient in fluid, $-(\partial P/\partial Z + \rho_w g \sin\alpha)$;
a, b, width and height of a rectangular channel, respectively;
C, axial temperature gradient, $\partial T/\partial Z$;
c_p, specific heat at constant pressure;
D_e, hydraulic diameter;
f, friction factor, $2\bar{\tau}_w/(\rho\bar{W}^2)$, or a dummy variable;
g, gravitational acceleration;
h, average heat-transfer coefficient;
k, thermal conductivity or kth outer iteration;
M, N, number of divisions in X and Y directions, respectively;
Nu, Nusselt number, hD_e/k;
n, dimensionless outward normal or nth inner iteration;
P, fluid pressure;
Pr, Prandtl number, ν/κ;
Ra, Rayleigh number, $g\beta CD_e^4/\nu\kappa$;
Ra^*, modified Rayleigh number, $Ra\sin\alpha$;
Ra_r^*, modified Rayleigh number for circular pipe based on radius $(g\beta Cr^4/\nu\kappa)\sin\alpha$;
Re_0, equivalent Reynolds number for Poiseuille flow with axial pressure gradient A and radius D_e, $AD_e^3/4\rho\nu^2$;
Re_0^*, modified Reynolds number, $Re_0\cot\alpha$;
Re_{0r}^*, modified Reynolds number for circular tube, $(Ar^3/4\rho\nu^2)\cot\alpha$;
T, local temperature;
U, V, W, velocity components in X, Y and Z directions, respectively;
u, v, w, dimensionless velocity components;
X, Y, Z, rectangular coordinates;
x, y, z, dimensionless coordinates, $(X, Y, Z)/D_e$.

Greek symbols

α, inclination angle from horizontal direction;
β, coefficient of thermal expansion;
γ, aspect ratio, a/b;
$\varepsilon_i, \varepsilon_0$, convergence criteria, equations (15) and (16);
θ, dimensionless temperature difference, $(T_w - T)/(Re_0 CD_e Pr)$;
κ, thermal diffusivity, $k/\rho c_p$;
μ, viscosity;
ν, kinematic viscosity, μ/ρ;
ξ, vorticity, $\nabla^2\psi$;
ρ, density;
τ, shear stress at wall;
ψ, dimensionless stream function;
ω, iteration parameter, equation (14);
∇^2, dimensionless Laplacian operator, $\partial^2/\partial x^2 + \partial^2/\partial y^2$.

Subscripts

b, bulk average;
i, j, location of a grid point in x and y directions;
0, pure forced convection;
w, value at wall.

Superscripts

k, n, kth outer iteration and nth inner iteration, respectively;
$\bar{}$, average value.

1. INTRODUCTION

COMBINED free and forced laminar convection in both vertical and horizontal circular tubes has been investigated theoretically and experimentally by many investigators for various conditions in recent years. In contrast, for the same problem in inclined tubes, a few theoretical studies [1–3] and only one experimental study [3] have been reported thus far in the literature. It is noted that these studies are concerned only with the case of fully developed velocity and temperature fields under the thermal boundary condition of axially uniform wall heat flux with peripherally uniform wall temperature. It is apparent that the inclination angle effect on the thermal convection has received relatively less attention in spite of its importance in practical applications such as flat plate solar collectors. Further-

more, one notes that the theoretical study on combined free and forced laminar convection in inclined rectangular channels appears to be nonexistent except for the limiting cases of vertical [4–6] and horizontal [7] orientations.

The purpose of this paper is to present flow and heat-transfer results for combined free and forced laminar convection problem with an upward flow in inclined rectangular channels under the axially uniform wall heat flux with a peripherally uniform wall temperature at any axial position for $Pr = 5$ and aspect ratios 0·5, 1, 2 by using an improved formulation. With the present formulation, only three independent parameters (Prandtl, modified Reynolds and Rayleigh numbers) appear explicitly in the governing equations for the fully developed combined free and forced convection in inclined channels. However, because of the introduction of modified Reynolds and Rayleigh numbers, the present formulation cannot recover the horizontal case as a limiting orientation.

For theoretical analysis of the combined free and forced convection in inclined tubes, the perturbation method [1, 3] is known to be valid for small Rayleigh number only and on the other hand the boundary layer approximation [3] appears to be useful only for large Rayleigh number regime. For the present problem in inclined rectangular channels, the analytical solution is apparently impractical and one must resort to numerical solution [2] for the coupled Navier–Stokes and energy equations.

When one considers the free convection effect on forced convection in inclined channels, one must distinguish between the cases of heating fluids flowing upward and cooling fluids flowing downward and those of heating with downflow and cooling with upflow. Depending on the situations indicated above, the axial component of the buoyancy force may coincide with main flow or be opposite to it. When buoyancy forces exist in the cross section normal to the main flow, a secondary flow appears.

For the case of negative Rayleigh number corresponding to the negative axial temperature gradient which is usually referred to as the case of heating from below, the thermal instability [4, 6] may arise. The instability problem is apparently outside the scope of present study. Although this investigation is concerned only with the buoyancy forces in gravitational field, the inclination angle effect may also arise under various situations involving buoyancy, centrifugal or Coriolis forces in rotating field. Since the inclination angle effects due to various body forces are similar, it is expected that the present method of solution is also applicable to a host of analogous problems involving other body forces.

2. ANALYSIS

Applying the usual assumptions of Boussinesq approximation, constant axial pressure gradient and neglecting viscous dissipation, the governing equations in rectangular coordinates (see Fig. 1) and the boundary conditions for hydrodynamically and thermally fully

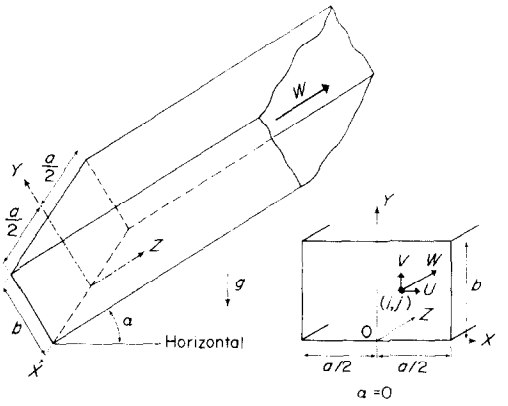

FIG. 1. Coordinate system for inclined rectangular channel.

developed steady laminar upward flow in an inclined rectangular channel subjected to a constant axial wall temperature gradient become:

Continuity equation

$$\frac{\partial U}{\partial X}+\frac{\partial V}{\partial Y}=0 \tag{1}$$

Momentum equations in X, Y and Z directions

$$U\frac{\partial U}{\partial X}+V\frac{\partial U}{\partial Y}=-\frac{1}{\rho}\frac{\partial P}{\partial X}+\nu\left(\frac{\partial^2 U}{\partial X^2}+\frac{\partial^2 U}{\partial Y^2}\right) \tag{2}$$

$$U\frac{\partial V}{\partial X}+V\frac{\partial V}{\partial Y}=-\frac{1}{\rho}\frac{\partial P}{\partial Y}+\nu\left(\frac{\partial^2 V}{\partial X^2}+\frac{\partial^2 V}{\partial Y^2}\right)+g\beta(T-T_w)\cos\alpha \tag{3}$$

$$U\frac{\partial W}{\partial X}+V\frac{\partial W}{\partial Y}=-\frac{1}{\rho}\frac{\partial P}{\partial Z}+\nu\left(\frac{\partial^2 W}{\partial X^2}+\frac{\partial^2 W}{\partial Y^2}\right)+g\beta(T-T_w)\sin\alpha-g\sin\alpha \tag{4}$$

Energy equation

$$U\frac{\partial T}{\partial X}+V\frac{\partial T}{\partial Y}+W\frac{\partial T}{\partial Z}=\kappa\left(\frac{\partial^2 T}{\partial X^2}+\frac{\partial^2 T}{\partial Y^2}\right) \tag{5}$$

Boundary conditions

$$U=V=W=T_w-T=0 \quad \text{at wall.} \tag{6}$$

After eliminating the pressure terms between the momentum equations in X and Y directions by cross-differentiation, the governing equations in the dimensionless form become:

Vorticity transport equation for secondary flow

$$\nabla^2\xi=u\frac{\partial\xi}{\partial x}+v\frac{\partial\xi}{\partial y}-Re_\delta^* Ra^*\frac{\partial\theta}{\partial x} \tag{7}$$

Stream function equation

$$\nabla^2\psi=\xi \tag{8}$$

Axial momentum equation

$$\nabla^2 w=u\frac{\partial w}{\partial x}+v\frac{\partial w}{\partial y}-4+Ra^*\theta \tag{9}$$

Energy equation

$$\nabla^2\theta = Pr\left(u\frac{\partial\theta}{\partial x}+v\frac{\partial\theta}{\partial y}\right)-w \tag{10}$$

Boundary conditions

$$\psi = w = \theta = 0 \quad \text{at wall} \tag{11}$$

$\psi = \xi = \partial\theta/\partial x = \partial w/\partial x = 0$ (symmetry) along vertical centerline where

$$X = (D_e)x, \quad Y = (D_e)y, \quad U = (\nu/D_e)u, \quad V = (\nu/D_e)v,$$
$$W = Re_0(\nu/D_e)w, \quad T_w - T = (Re_0 CD_e Pr)\theta,$$
$$\partial T/\partial Z = C, \quad A = -(\partial P/\partial Z + \rho_w g\sin\alpha),$$
$$Re_0 = AD_e^3/4\rho\nu^2, \quad Pr = \nu/\kappa, \quad Ra = g\beta CD_e^4/\nu\kappa,$$
$$P = \rho(\nu/D_e)^2 p, \quad Re = \overline{W}D_e/\nu = Re_0\overline{w},$$
$$Re_\delta^* = Re_0\cot\alpha, \quad Ra^* = Ra\sin\alpha, \quad u = \partial\psi/\partial y$$
$$\text{and } v = -\partial\psi/\partial x \tag{12}$$

It is seen that with the introduction of modified Reynolds and Rayleigh numbers, Re_δ^* and Ra^* the inclination angle from the horizontal direction α does not appear explicitly in the formulation. Noting that $\sin\alpha$ and $\cot\alpha$ approach 0 and ∞ respectively as $\alpha \to 0°$, it is clear that the limiting case of horizontal channel $\alpha = 0°$ must be excuded from the present formulation. The number of independent parameters becomes three in contrast to four for the earlier formulation [1, 2].

The expressions for the usual flow and heat-transfer results, fRe and Nu, can be obtained in two alternative forms by considering the normal wall gradients or overall force and energy balance as

$$(fRe)_1 = 2(\overline{\partial w}/\partial n)_w/\overline{W}, \quad (fRe)_2 = (2/\overline{w})[1-(Ra^*\overline{\theta}/4)]$$
$$(Nu)_1 = -(\overline{\partial\theta}/\partial n)_w/\theta_b, \quad (Nu)_2 = \overline{w}/4\theta_b. \tag{13}$$

3. NUMERICAL SOLUTION

The three-point central difference formula is applied to all the derivatives. As pointed out in [2], the combination of boundary vorticity method and line iteration method can be employed for the numerical solution of the two coupled elliptic-type equations (7) and (8). For this study, the ADI algorithm [8] is used in solving equations (9) and (10). The iteration parameter ω used in the ADI method is the one based on linear equation.

$$\omega = 4\sin(\pi/2N)\cos(\pi/2N) \tag{14}$$

where N is the total number of nodal points in y direction. The convergence criterion for the inner iterations of ξ, ψ, w and θ is defined as follows using a dummy variable f.

$$\varepsilon_i = \sum_{i,j}|f_{i,j}^{(n+1)} - f_{i,j}^{(n)}|/\sum_{i,j}|f_{i,j}^{(n+1)}| < 10^{-4} \tag{15}$$

where n represents nth inner iteration. The outer iterations are checked only for w and θ by the following criterion.

$$\varepsilon_0 = \sum_{i,j}|f_{i,j}^{(k+1)} - f_{i,j}^{(k)}|/\sum_{i,j}|f_{i,j}^{(k+1)}| < 10^{-3} \tag{16}$$

where k stands for kth outer iteration. Numerical experiments reveal that the above decision procedure (based on the use of average deviation of a variable from the previous iteration over the grid matrix) for terminating the iterations gives reasonable accuracy for such quantities as friction factor and Nusselt number.

Briefly, for given values of Pr, Re_δ^* and Ra^* the numerical solution proceeds as follows:

1. Assign the initial values for u, v, w, θ, ψ and ξ. Equations (7) and (8) are iterated until the convergence criterion $\varepsilon_i < 10^{-4}$ is satisfied.
2. By using the updated secondary flow velocity components u and v, the axial momentum equation (9) is iterated until equation (15) is satisfied.
3. Perform the same iteration as step 2 for energy equation (10). One complete outer iteration is thus completed.
4. Repeat steps 1 to 3 until equation (16) is satisfied.

After obtaining a convergent solution, the flow and heat-transfer results, fRe and Nu, are evaluated using Simpson's rule for numerical integration. The grid sizes of $M \times N = 10 \times 20$, 16×16 and 8×32 are used for $\gamma = 1$, 2 and 0·5, respectively. The accuracy of the numerical solution can be assessed by comparing the numerical results for fRe and Nu using two alternative expressions. In the present study, the agreement between the two alternative results is excellent when Ra^* is small but the difference increases with the further increase of Ra^*. It is believed that with the grid size of 10×20 for $\gamma = 1$, for example, the numerical evaluation of $\partial w/\partial n$ and $\partial\theta/\partial n$ at wall leads to some error. Thus, one may conclude that with the grid sizes used in this study, the numerical results from $(fRe)_2$ and $(Nu)_2$ are more accurate and will be used in the presentation of results. The maximum deviation of $(fRe)_1$ and $(Nu)_1$ from $(fRe)_2$ and $(Nu)_2$, respectively, is about 7 per cent at the highest Ra^* investigated. For the case of vertical channels, the exact solution for the present problem is given in [6] and is used in checking the convergence and accuracy of the numerical solution. For the case of vertical square channel, the Nusselt numbers from this analysis agree excellently with the recalculated values [9] for the results given in Table 3 of [6]. For given values of γ, Pr, Ra^* and Re_δ^*, the computing time required for a complete solution is generally less than one minute on the IBM 360/67 system.

4. FLOW AND HEAT-TRANSFER RESULTS

In this study, the numerical calculations are carried out for Prandtl number 5 only. The axial velocity and temperature profiles along $x = 0$ and $y = 0·5$ are shown in Figs. 2 and 3, respectively, with Ra^* as parameter for $Pr = 5$ and $Re_\delta^* = 500$. The effect of Ra^* on the behavior of axial velocity profiles $x = 0$ is similar to that of inclined tube case as shown in Fig. 2(a) of [2] and can be explained similarly [2] by considering the relative magnitude of the terms $v\partial w/\partial y$ and $Ra^*\theta$ on the RHS of axial momentum equation (9). In this connection, the membrane analogy may be used in explaining a back flow phenomenom. For the present case of upward flow with heating, the term $Ra^*\theta$ is positive and the back flow may occur when the RHS of equation (9) becomes positive in some region as indicated by the curves for $Ra^* = 10^4$ in Fig. 2. At $Ra^* = 10^4$

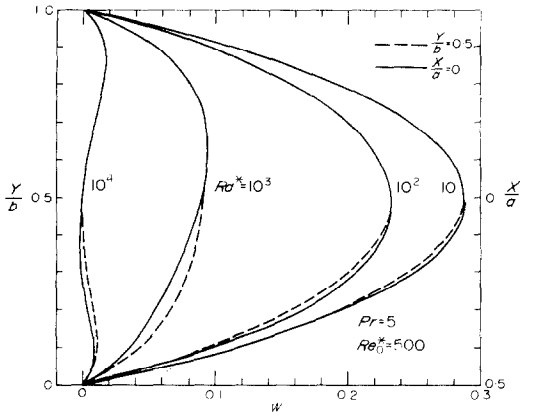

FIG. 2. Effect of Ra^* on axial velocity profile along $x = 0$ and $y = 0{\cdot}5$ for $\gamma = 1$, $Pr = 5$ and $Re_\delta^* = 500$.

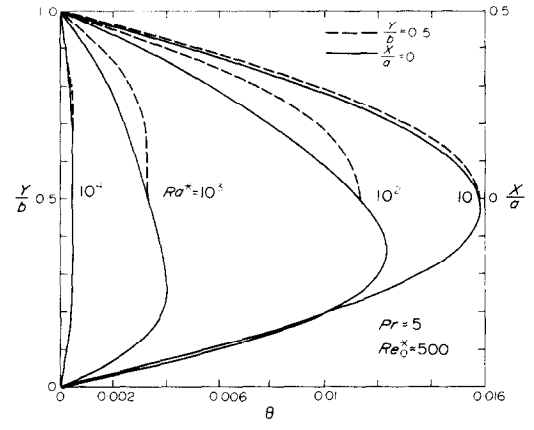

FIG. 3. Effect of Ra^* on temperature profile along $x = 0$ and $y = 0{\cdot}5$ for $\gamma = 1$, $Pr = 5$ and $Re_\delta^* = 500$.

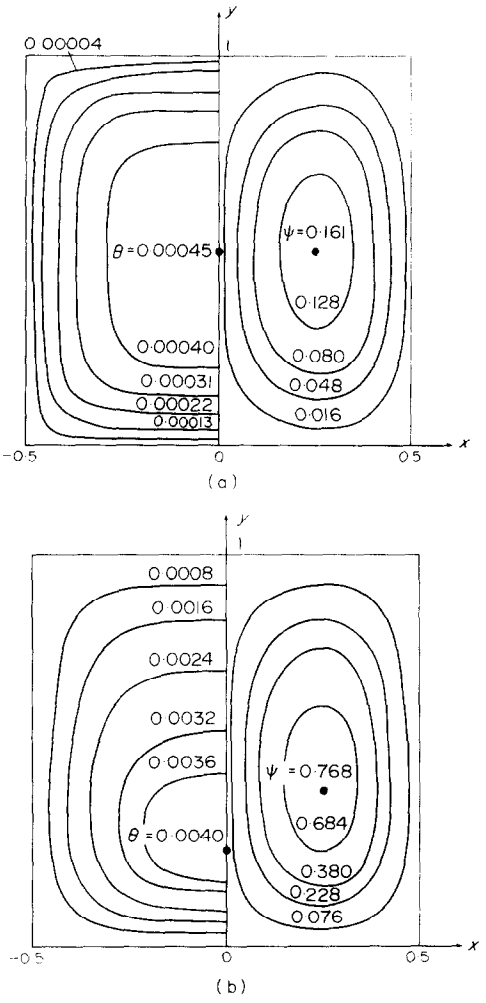

FIG. 4. Streamline and isotherm patterns for (a) $\gamma = 1$, $Pr = 5$, $Re_\delta^* = 100$, $Ra^* = 10^4$ and (b) $\gamma = 1$, $Pr = 5$, $Re_\delta^* = 500$, $Ra^* = 10^3$.

the back flow already appears and the temperature profile is fairly uniform over the whole cross section. For the cases $Re_\delta^* = 0$, 5, 50, 100 and 500 with $\gamma = 1$, 2 and 0·5 considered in this study, the back flow is found to occur when Ra^* is between 7×10^3 and 8×10^3. However, no attempt was made to determine the exact values for Ra^*.

In the vorticity transport equation (7) for secondary flow, the driving term is the term involving $\partial\theta/\partial x$ and this term is seen to be very small in the core region for the profile $Ra^* = 10^4$ shown in Fig. 3. It is seen that the secondary flow is rather weak at $Ra^* = 10^4$. Further insight may be obtained by inspecting the streamline and isotherm patterns for $\gamma = 1$ and $Pr = 5$ shown in Figs. 4 (a) and (b) for $Re_\delta^* = 100$, $Ra^* = 10^4$ and $Re_\delta^* = 500$, $Ra^* = 10^3$, respectively. One notes that Fig. 4(b) corresponds to the profiles $Ra^* = 10^3$ shown in Figs. 2 and 3. The maximum value of the stream function at the eye of the vortices may be regarded to represent the intensity of secondary flow. At $Re_\delta^* = 100$, $Ra^* = 10^4$, the intensity of the secondary flow is seen to be considerably weaker than that at $Re_\delta^* = 500$ and $Ra^* = 10^3$. One also notes the different locations for the eye of vortices and the maximum magnitude for θ. This situation is similar to the difference between the profiles for $Ra^* = 10^4$ and 10^3 shown in Fig. 3. Thus, it is well to note that Ra^* does not necessarily represent the buoyancy force effect. At very high values of Ra^*, the magnitudes of w and θ become rather small and this fact coupled with the back flow may be the cause of numerical difficulty.

The friction factor and Nusselt number results are of practical interest in design. For $\gamma = 1$ and $Pr = 5$, the flow and heat-transfer results are shown in Figs. 5 and 6, respectively, with Re_δ^* as parameter. For inclined channels, both the aiding buoyancy force and secondary flow effects exist and the interaction occurs. For a given Re_δ^* the product fRe is seen to increase with Ra^* and an asymptotic behavior seems to appear at $Ra^* = 10^4$. Practically, the effect of Re_δ^* is seen to be confined only to the range $Ra^* = 10^2$–10^4 and for a given Ra^* the product fRe decreases with the increase of Re_δ^* which is a known fact. For $Re_\delta^* \lesssim 100$, the effect of Re^* on friction factor result is apparently negligible. On the other hand, with $Ra^* \gtrsim 10^4$, the friction factor result is seen to be independent of Re_δ^*.

From Fig. 6, one can see the effects of Re_δ^* and Ra^* on Nusselt number. The effect of Re_δ^* on Nu is negligible when $Re_\delta^* < 100$. Furthermore, the effect of

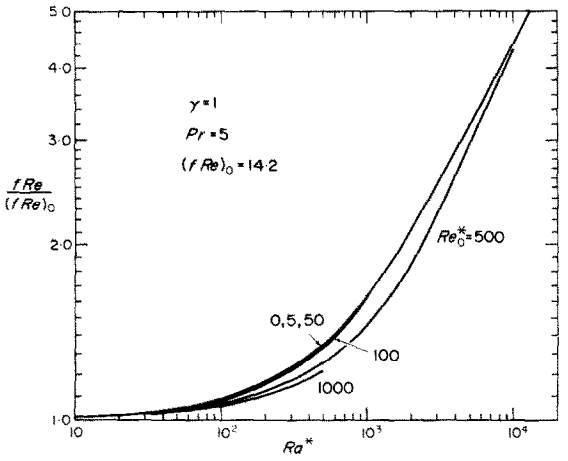

FIG. 5. $fRe/(fRe)_0$ vs Ra^* with Re_δ^* as parameter for $\gamma = 1$, $Pr = 5$.

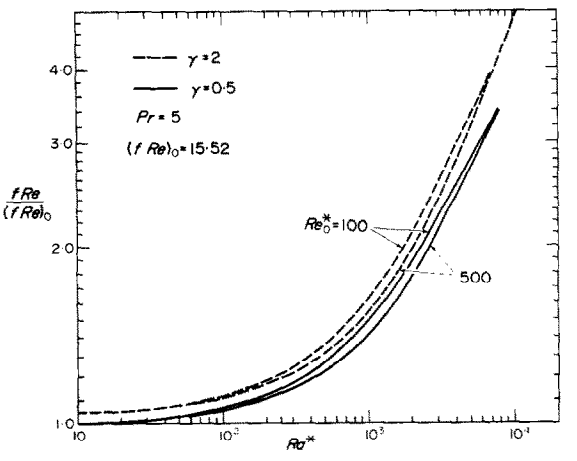

FIG. 7. $fRe/(fRe)_0$ vs Ra^* with Re_δ^* as parameter for $\gamma = 0{\cdot}5$, 2 and $Pr = 5$.

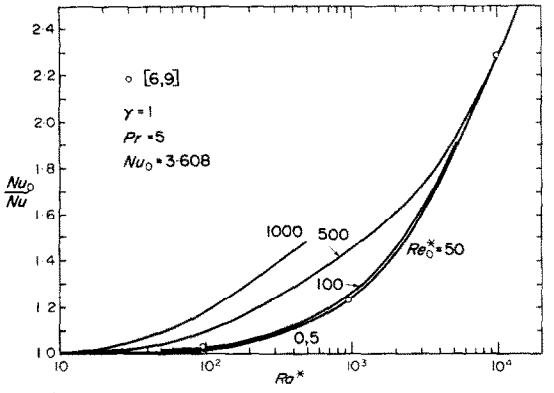

FIG. 6. $Nu/(Nu)_0$ vs Ra^* with Re_δ^* as parameter for $\gamma = 1$, $Pr = 5$.

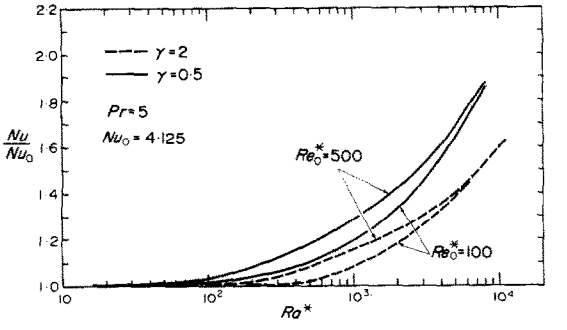

FIG. 8. $Nu/(Nu)_0$ vs Ra^* with Re_δ^* as parameter for $\gamma = 0{\cdot}5$, 2 and $Pr = 5$.

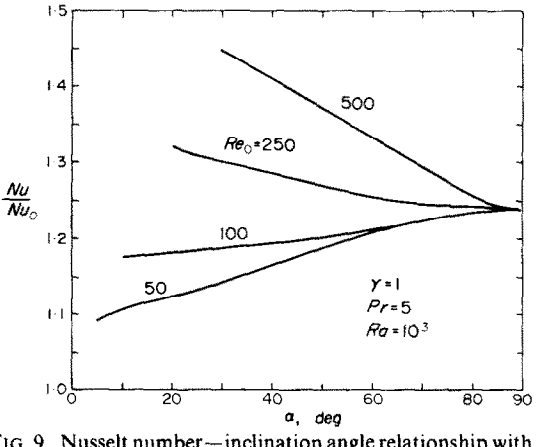

FIG. 9. Nusselt number—inclination angle relationship with Re_0 as parameter for $\gamma = 1$, $Pr = 5$ and $Ra = 10^3$.

Re_δ^* on Nu is confined to the range $10 < Ra^* < 6 \times 10^3$. With $Ra^* > 10^4$, the asymptotic behavior appears. As noted earlier, the analytical results [6, 9] are available in the literature for the case of vertical square channel $Re_\delta^* = 0$ and are plotted in Fig. 6 for comparison. The agreement is seen to be excellent.

In order to study the aspect ratio effect, flow and heat-transfer results are shown in Figs. 7 and 8, respectively, for $Pr = 5$ and $\gamma = 0{\cdot}5$, 2. The general behavior is quite similar to that of $\gamma = 1$. The results show that the aspect ratio $\gamma = 0{\cdot}5$ (narrow and tall channel) is superior to $\gamma = 2$ (thin and flat channel) from the viewpoint of both friction factor and heat transfer rate under the same conditions. The explanation for the behavior cannot be made readily since the expressions for $(fRe)_1$ and $(Nu)_1$ for example, involve $\overline{\partial w}/\partial n$, $\bar{w}$ and $\overline{\partial\theta}/\partial n$, $\bar{\theta}_b$, respectively. For narrow and tall channels, one would expect greater free convection effect from the side walls.

In the present formulation, the inclination angle effect appears only implicitly through the parameters Re_δ^* and Ra^*. However, the present results may be used to elucidate the inclination angle effect and the derived results based on Fig. 6 are illustrated in Fig. 9 where the Nusselt number is plotted against inclination angle α with Re_0 as parameter for $\gamma = 1$, $Pr = 5$ and $Ra = 10^3$. The effect of Re_0 on Nu–α relationship is seen to be qualitatively similar to that shown in Fig. 14 of [2] for the case of inclined circular tubes. Noting that $\cot\alpha \to \infty$ as $\alpha \to 0$ for the parameter Re_δ^*, one can readily understand that the Nusselt number result is not available near horizontal orientation depending on the value of Re_0. Figure 9 also shows that the inclination angle effect is considerably more significant near the horizontal orientation $\alpha = 0°$ than that near the vertical position $\alpha = 90°$.

In view of the generalized nature of the present formulation, it is desirable to present flow and heat-transfer results for the case of inclined circular tubes

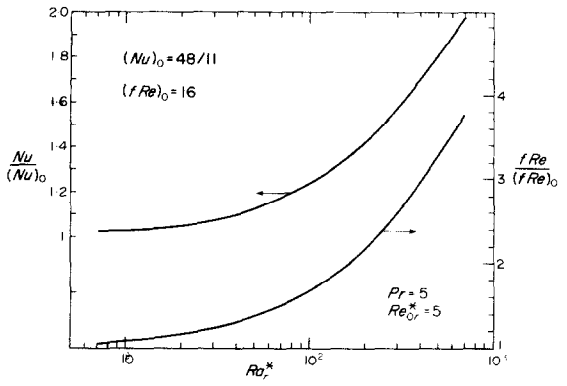

FIG. 10. $Nu/(Nu)_0$ and $fRe/(fRe)_0$ vs Ra_r^* relationship for inclined circular tubes with $Pr = 5$ and $Re^*_{0r} = 5$ from [10].

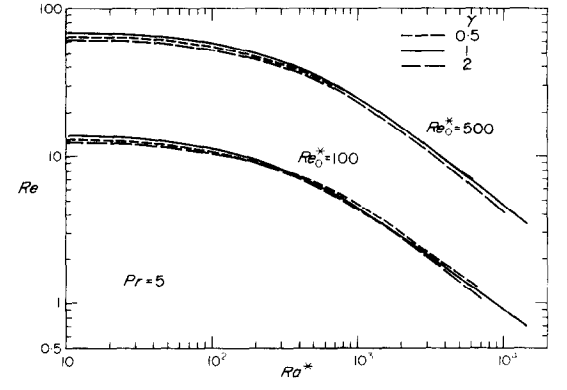

FIG. 11. Re–Ra^* relationship for $Re_0^* = 100$, 500 with $\gamma = 0{\cdot}5$, 1, 2 and $Pr = 5$.

using the parameters corresponding to Re_0^* and Ra^*. For this purpose, the results from Figs. 2 and 3 of [10] are transformed into those shown in Fig. 10 using the parameters Re^*_{0r} and Ra_r^*.

For practical application in design, one may wish to compute the Reynolds number, Re, corresponding to given Re_0^* and Ra^*. For this purpose the example cases of $Re_0^* = 100$ and 500 with $Pr = 5$ and $\gamma = 0{\cdot}5$, 1, 2 are illustrated in Fig. 11. It is found that the value of $\bar{w}$ is rather insensitive with respect to Re_0^* and γ.

CONCLUDING REMARKS

1. The present study shows that it is not required to carry out the numerical solution for each inclined angle in order to study the inclination angle effects. The Nusselt number for fully developed flow conditions is greatly influenced by the inclination angle effect and Re_0 near the horizontal direction as shown in Fig. 9.

2. The present numerical results for the limiting case of vertical channels agree with the analytical results [6, 9] which in turn have been confirmed by experimental results shown in Fig. 3 of [11] for $\gamma = 0{\cdot}1$. In view of the agreement between theory [6] and experiment [11], and also the range of the experimental data shown in Fig. 15 of [3], one may also deduce that the range of Ra^* (0–10^4) investigated is practical.

3. For higher Ra^*, the question regarding the effect of natural convection on stability of laminar flow arises. The instability data and heat-transfer result in the transition regime for combined free and forced convection in inclined tubes or channels do not seem to be available.

Acknowledgement—This work was supported by the National Research Council of Canada through grant NRC A1655.

REFERENCES

1. M. Iqbal and J. W. Stachiewicz, Influence of tube orientation on combined free and forced laminar convection heat transfer, *J. Heat Transfer* **88**, 109–116 (1966).
2. K. C. Cheng and S. W. Hong, Combined free and forced laminar convection in inclined tubes, *Appl. Scient. Res.* **27**, 19–38 (1972).
3. K. Futagami and F. Abe, Combined forced and free convective heat transfer in an inclined tube (1st report, laminar region), *Trans. Japan. Soc. Mech. Engrs* **38**(311), 1799–1811 (1972).
4. S. Ostrach, Combined natural and forced-convection laminar flow and heat transfer of fluids with and without heat sources in channels with linearly varying wall temperatures, NACA TN3141 (1954).
5. L. S. Han, Laminar heat transfer in rectangular tubes with combined free and forced-convection, *J. Am. Soc. Naval Engrs* **67**, 163–167 (1955).
6. L. S. Han, Laminar heat transfer in rectangular channels, *J. Heat Transfer* **81**, 121–128 (1959).
7. K. C. Cheng and G. J. Hwang, Numerical solution for combined free and forced laminar convection in horizontal rectangular channels, *J. Heat Transfer* **91**, 59–66 (1969).
8. D. Young, The numerical solution of elliptic and parabolic partial differential equations, in *Survey of Numerical Analysis*, edited by J. Todd, pp. 380–438. McGraw-Hill, New York (1962).
9. M. Iqbal, S. A. Ansari and B. D. Aggarwala, Effect of buoyancy on forced convection in vertical regular polygonal ducts, *J. Heat Transfer* **92**, 237–244 (1970).
10. K. C. Cheng and S. W. Hong, Effect of tube inclination on laminar convection in uniformly heated tubes for flat-plate solar collectors, *Solar Energy* **13**, 363–371 (1972).
11. A. K. Muntjewerf, H. A. Leniger and W. J. Beek, An experimental investigation of heat transfer to laminar Newtonian flows in uniformly heated vertical flat rectangular ducts, *Appl. Scient. Res.* **23**, 134–146 (1970).

CONVECTION MIXTE LAMINAIRE DANS DES CANAUX RECTANGULAIRES INCLINES

Résumé—On étudie la convection mixte laminaire naturelle et forcée en régime établi avec écoulement ascendant dans des canaux rectangulaires inclinés avec des conditions aux limites thermiques à flux constant à la paroi ou à gradient pariétal de température constant. L'étude est faite à l'aide d'une méthode numérique utilisant une formulation améliorée dans laquelle trois paramètres physiques indépendants Pr, Re_0^*, Ra^*, apparaissent au lieu de quatre comme dans les expériences précédentes relatives à des tubes circulaires inclinés. Les résultats numériques relatifs au coefficient de frottement et au nombre de

Nusselt sont présentés pour $Pr = 5$ et pour des rapport de section $\gamma = 0{,}5$–1–2. Les nouveaux paramètres sont également utilisés pour corréler les résultats antérieurs dynamiques et thermiques pour les tubes inclinés. On trouve que l'effet de l'angle d'inclinaison est plus important autour de la position horizontale et qu'il decroit lorsqu'on approche de la position verticale. Aux nombres de Rayleigh Ra^* élevés, par exemple $Ra^* = 10^4$, pour $\gamma = 1$ et $Pr = 5$, l'écoulement et le transfert de chaleur deviennent indépendants de Re_δ^* et un comportement asymptotique apparait.

KOMBINIERTE FREIE UND ERZWUNGENE KONVEKTION IN GENEIGTEN, RECHTECKIGEN KANÄLEN

Zusammenfassung—Es wird die voll ausgebildete, kombinierte freie und erzwungene laminare Konvektion bei Aufwärtsströmung in geneigten, rechteckigen Kanälen untersucht mit der Grenzbedingung axial einheitlichen Wärmeflusses oder konstanten Wandtemperatur-Gradienten. Dafür wird eine verbesserte numerische Methode benützt, in der drei unabhängige physikalische Parameter Pr, Re_δ^*, Ra^* auftreten anstelle von vier wie in den früheren Untersuchungen an geneigten kreisförmigen Rohren. Numerische Ergebnisse für die Reibung und die Nusselt–Zahl werden angegeben für $Pr = 5$ und Längenverhältnisse $\gamma = 0{,}5$; 1; 2. Die neuen Parameter werden auch herangezogen zu Korrelationen früherer Ergebnisse in geneigten Rohren. Der Einfluß des Neigungswinkels ist besonders stark in der Nähe der horizontalen Lage und nimmt ab mit zunehmender Senkrechtstellung. Bei Ra^*, z.B. $Ra^* = 10^4$ für $\gamma = 1$, $Pr = 5$, werden die Ergebnisse für die Strömung und den Wärmeübergang unabhängig von Re_δ^*, und es tritt das asymptotische Verhalten auf.

СОВМЕСТНАЯ СВОБОДНАЯ И ВЫНУЖДЕННАЯ ЛАМИНАРНАЯ КОНВЕКЦИЯ В НАКЛОННЫХ КАНАЛАХ ПРЯМОУГОЛЬНОГО СЕЧЕНИЯ

Аннотация — Полностью развитая и вынужденная ламинарная конвекция при восходящем течении в наклонных каналах прямоугольного сечения при тепловых пограничных условиях однородного вдоль оси пристенного теплового потока или постоянного пристенного градиента температур изучается с помощью численного метода. Применяется исправленная формулировка, в которую вместо четырех независимых физических параметров, используемых в более ранних исследованиях по наклонным трубам круглого сечения, входят три параметра Pr, Re_0^* и Ra^*. Числовые данные для коэффициента трения и числа Нуссельта приводятся при $Pr = 5$ и отношений характерных размеров $\gamma = 0{,}5$, 1,2. Новые параметры используются также для корреляции ранее полученных данных для течений и теплообмена в наклонных трубах. Найдено, что влияние угла наклона наиболее сильно сказывается в области горизонтальной ориентации и уменьшается по приближении к вертикальному направлению. При более высоких Ra^*, например, $Ra^* = 10^4$, $\gamma = 1$, $Pr = 5$ данные по течению и теплообмену становятся не зависимыми от Re_0^* и начинают проявлять асимптотическое поведение.